

Prediction and Prevention of Pandemics via Graphical Model Inference and Convex Programming

Mikhail Krechetov¹, Amir Mohammad Esmiaeeli Sikaroudi², Alon Efrat^{2,3}, Valentin Polishchuk⁴,
and Michael Chertkov^{3,5,2,1}

¹ Skolkovo Institute of Science and Technology, Moscow, Russia, 121205

² Department of Computer Science, University of Arizona, Tucson, AZ, USA, 85721

³ Program in Applied Mathematics, University of Arizona, Tucson, AZ, USA, 85721

⁴ Linkoping Univeristy, Norrkoping, Sweden, 60174

⁵ Department of Mathematics, University of Arizona, Tucson, AZ, USA, 85721

Mikhail.Krechetov@skoltech.ru, chertkov@arizona.edu

Abstract

Hard-to-predict bursts of COVID-19 pandemic revealed significance of statistical modeling which would resolve spatio-temporal correlations over geographical areas, for example spread of the infection over a city with census tract granularity. In this manuscript, we provide algorithmic answers to the following two **inter-related public health challenges of immense social impact which have not been adequately addressed by the AI community**. (1) **Inference Challenge**: assuming that there are N census blocks (nodes) in the city, and given an initial infection at any set of nodes, e.g. any N of possible single node infections, any $N(N-1)/2$ of possible two node infections, etc, what is the probability for a subset of census blocks to become infected by the time the spread of the infection burst is stabilized? (2) **Prevention Challenge**: What is the minimal control action one can take to minimize the infected part of the stabilized state footprint? To answer the challenges, we build a Graphical Model of pandemic of the attractive Ising (pair-wise, binary) type, where each node represents a census track and each edge factor represents the strength of the pairwise interaction between a pair of nodes, e.g. representing the inter-node travel, road closure and related, and each local bias/field represents the community level of immunization, acceptance of the social distance and mask wearing practice, etc. **Resolving the Inference Challenge** requires finding the Maximum-A-Posteriori (MAP), i.e. most probable, state of the Ising Model constrained to the set of initially infected nodes. (An infected node is in the $+1$ state and a node which remained safe is in the -1 state.) We show that almost all attractive Ising Models on dense graphs result in either of the two possibilities (modes) for the MAP state: either all nodes which were not infected initially became infected, or all the initially uninfected nodes remain uninfected (susceptible). This bi-modal solution of the Inference Challenge allows us to re-state the **Prevention Challenge** as the following **tractable convex programming**: for the bare Ising Model with pair-wise and bias factors representing the system without prevention measures, such that the MAP state is fully infected for at least one of the initial infection patterns, find the closest, in l_1 norm, therefore prevention-optimal, set of factors resulting in all the MAP states of the Ising model, with the optimal prevention measures applied, to become safe.

Introduction: Graphical Models of Pandemics

We follow our previous work (Chertkov et al. 2021) in justification for the use of the Graphical Models (GM) to study and mitigate pandemics. Therefore, we start from providing a brief recap of the prior literature on modeling of the epidemics, describe the logic which led us in (Chertkov et al. 2021) to the Ising Model (IM) formulation, and then state formally the inference and prevention problems addressed in the manuscript.

Difficulty in both predicting and neutralizing the spread of pandemics is a major social challenge of humanity. Technically speaking, we are yet to design a coherent data lifecycle for modeling and prevention both in terms of the global strategies and local tactics. To address the challenge, we must devise a hierarchy of spatio-temporal models with different resolutions – from individual to community, county to the city, and from the moment a pathogen first enters our bodies, to days of disease development and to community transmission. Importantly, the models should be efficient in computing probabilistic predictions (for instance, offering the marginal probability heat map for the city neighborhoods to transition from the current/prior state of infection to the projected/a-posteriori state in two weeks).

Epidemiology and Mathematical Biology experts have relied in the past on a number of modeling approaches. The Agent-Based-Models (ABMs), introduced in epidemiology in 2004-2008 (Eubank et al. 2004; Longini et al. 2005; Ferguson et al. 2005, 2006; Germann et al. 2006; Halloran et al. 2008), have complemented the earlier compartmental models (Ross 1910; Kermack, McKendrick, and Walker 1927; Anderson and May 1991; Hethcote 2000). Using ABMs, even though not exclusive to epidemiology (Wikipedia 2020; Downey 2018), became a breakthrough in the field, as they allowed to make a significant improvement in the quality of predictions, especially in the spatio-temporal resolution of how the disease spreads and how one can mitigate its spread. The models became and remained a core part of the epidemiology data life-cycle. (See for instance (Lovasi and et.al. 2020; Kerr et al. 2021) for most recent bibliography.) The ABMs provide a detailed prediction of how pandemics spread within counties, cities, and regions. A majority of the country-, city- or county-

scale testbeds testing various mitigation strategies are resolved nowadays with ABMs. In particular, recently ABMs have been used extensively to inform public health in (non-pharmaceutical) interventions against the spread of COVID-19 (Ferguson et al. 2020; Eubank et al. 2020; LANL 2020; Maziarz and Zach 2020; Kaxiras and Neofotistos 2020), and verify new strategies like test-trace-quarantine (Kerr et al. 2021), among many other applications.

There are two major problems with the modeling of pandemic. First, many parameters need to be calibrated on data. Second, even when calibrated for the current state of pandemic the models which are too detailed become impractical for making a forecast and for developing prevention strategies – both requiring checking multiple (forecast and/or prevention) scenarios. Using ABMs, which are clearly over-modeled (too detailed) is especially problematic in the context of the latter. For example, the open-source ABM solver FLUTE (Chao et al. 2010) developed originally for modeling influenza, works with data that are acquired through Geographic Information Systems (GIS) on the scale of census tracts or communities, which is a very reasonable scale of spatial resolution to understand the dynamics of pandemics on a local scale. FLUTE populates each of the communities with thousands to millions of inhabitants in order to account for their daily patterns of travel. We believe that constructing effective Graphical Models (GM) of Pandemics with community-scale spatial resolution and then modeling pairwise (and possibly higher-order) epidemic interactions between communities directly, without introducing the thousands-to-millions of dummy agents, will complement (as discussed in the next paragraph), but also improve upon ABMs by being more efficient, robust and easier to calibrate.

An important, and possibly one of the first, Graphical Model (GM) of the COVID-19 pandemic was proposed in (Chang et al. 2020). Dynamic bi-partite GMs connecting census tracts to specific Points Of Interest (non-residential locations that people visit such as restaurants, grocery stores and religious establishments) within the city and studying dynamics of the four-state (Susceptible, Exposed, Infectious and Removed) of a census tract (graph node) on the graph, were constructed in (Chang et al. 2020) for major metro-area in USA based on the SafeGraph mobility data (SafeGraph 2021).

In fact, similar dynamic GMs, e.g. of the Independent Cascade Model (ICM) type (Kempe, Kleinberg, and Tardos 2003; Netrapalli and Sanghavi 2012; Gomez-Rodriguez, Leskovec, and Krause 2012; Khalil, Dilikina, and Song 2013; Rosenfeld, Nitzan, and Globerson 2016), were introduced even earlier in the CS/AI literature in the context of modeling how the rumors spread over social networks (with a side reference on using ICM in epidemiology). As argued in (Chertkov et al. 2021) the Independent Cascade Models (ICMs) can be adapted to modeling pandemics. (Another interesting use of the ICM to model COVID-19 pandemic was discussed in (Chen et al. 2020).) In its minimal version, an ICM of Pandemic can be built as follows. Assume that the virus spreads in the community (census tract) sufficiently fast, say within five days – which is the estimate for the early versions of COVID-19 median in-

cupation period. If an infected person enters a community/neighborhood but does not stay there, he infects others with some probability. If a single resident of the community becomes infected, all other residents are assumed infected as well (instantaneously). The model is a discrete-time dynamic model in which nodes in a network are in one of the three states: **S**usceptible, **I**nfected, or **R**emoved. The nodes represent communities/neighborhoods. A contact between an **I**nfected community/node and another community which is **S**usceptible has an assigned probability of disease transmission, which can also be interpreted as the probability of turning the **S** state into **I** state. Consistently with what was described above, the network is represented as a graph, where nodes are tracts and edges, connecting two tracts, have an associated strength of interaction representing the probability for the infection to spread from one node to its neighbor. A seed of the infection is injected initially at random, for example, mimicking an exogenous super-spreader infection event in the area; examples could include political or religious gatherings. See Figure 1 illustrating dynamics of the cascade model over 3-by-3 grid graph. Color coding of nodes is according to **S**usceptible=blue, **I**nfected=red, **R**emoved=black. Given the starting infection configuration, each infected community can infect its graph-neighbor community during the next time step with the probability associated with the edge connecting the two communities. Then the infected community moves into the removed state. The attempt to infect each neighbor is independent of all other neighbors. This creates a cascading spread of the virus across the network. The cascade stops in a finite number of steps, thereby generating a random **R**emoved pattern, shown in black in the Fig. 1, while other communities which were never infected (remain **S**usceptible) are shown in blue.

It was shown in (Chertkov et al. 2021) that with some regularization applied, statistics of the terminal state of the Cascade Model of Pandemic turns into a Graphical Model of the attractive Ising Model type.

This manuscript Road Map. Working with the Ising Model of Pandemic, we start the technical part of the manuscript by posing the **Inference/Prediction Challenge** in Section 1. Here, the problem is stated, first, as the Maximum A-Posteriori over an attractive Ising Model, and we argue, following the approach which is classic in the GM literature, that problem can be re-stated as a tractable LP. We then proceed to Section 2 to pose the main challenge addressed in the manuscript – the **Prevention Challenge** – as the two-level optimization with inner step requiring resolution of the aforementioned Prediction Challenge. Aiming to reduce the complexity of the Prevention problem, we turn in Section 3 to the analysis of the conditions in the formulation of the Prediction Challenge, describing the Safety domain in the space of the Ising Model parameters. We show the Safety domain is actually a polytope, even though exponential in the size of the system. We proceed in Section 5 with analysis of the Prevention Challenge, discussing the interpretation of the problem as a projection to the Safety Polytope from the polytope exterior, needed when the bare prediction suggests that system will be found with high probability outside of the Safety Polytope. Section 4 is devoted to

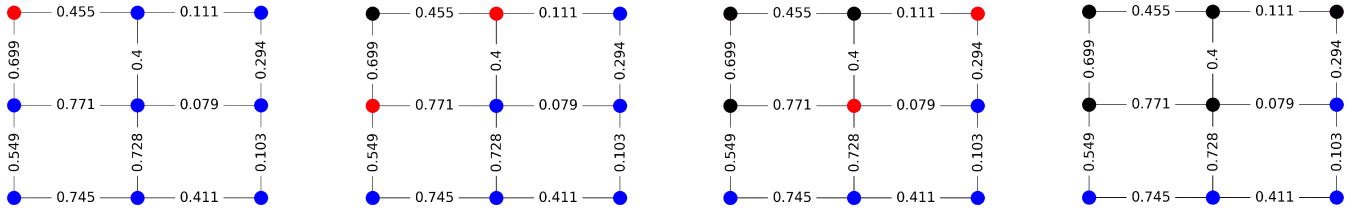


Figure 1: An exemplary random sequence (top-left to top-right to bottom-left to bottom-right) of the Independent Cascade Model (ICM) dynamics over 3×3 grid. Nodes colored red, blue, and black are **I**nfected, **S**usceptible, and **R**emoved at the respective stage of the dynamical process. This (shown) sample of the dynamic process terminates in 3 steps. Ising Model of Pandemic (IMP), which is the focal point of this manuscript, describes a regularized version of the ICM terminal state, where only two states (**S**-blue and **R**-black) are left. (See text for details.)

approximation which allows an enormous reduction in the problem complexity. We suggest here that if the graph of the system is sufficiently dense, the resulting MAP solution may only be in one of the two polarized states (a) completely safe (no other nodes except the initially infected) pick the infection, or (b) the infection is spread over the entire system. We support this remarkable simplification by detailed empirical analysis and also by some theoretical arguments. Section 6 is devoted to the experimental illustration of the methodology on the practical example of the Graphical Model of Seattle. The manuscript is concluded in Section 7 with a brief summary and discussion of the path forward.

1 Ising Model of Pandemic

As argued in (Chertkov et al. 2021) the terminal state of a dynamic model generalizing the ICM model can be represented by the Ising Model of Pandemic (IMP), defined over graph $\mathcal{G} = (\mathcal{V}, \mathcal{E})$, where \mathcal{V} is the set of $N = |\mathcal{V}|$ nodes and \mathcal{E} is the set of undirected edges. The IMP, parameterized by the vector of the node-local biases, $h = (h_a | a \in \mathcal{V}) \in \mathbb{R}^N$, and by the vector of the pair-wise (edge) interactions, $J = (J_{ab} | \{a, b\} \in \mathcal{E})$, describes the following Gibbs-like probability distribution for a state, $x = (x_a = \pm 1 | a \in \mathcal{V}) \in 2^{|\mathcal{V}|}$, associated with \mathcal{V} :

$$P(x | J, h) = \frac{\exp(-E(x | J, h))}{Z(J, h)}, \quad (1)$$

where any node, $a \in \mathcal{V}$ can be found in either **S**- (susceptible, never infected) state, marked as $x_a = -1$, or **R**- (removed, i.e. infected prior to the termination) state, marked as $x_a = +1$. In Eq. (1), $E(x | J, h)$ and $Z(J, h)$ are model's energy function and partition function respectively:

$$E(x | J, h) = \sum_{a \in \mathcal{V}} h_a x_a - \sum_{a, b \in \mathcal{V}} J_{ab} x_a x_b, \quad (2)$$

$$Z(J, h) = \sum_x \left(\sum_{a \in \mathcal{V}} h_a x_a - \sum_{a, b \in \mathcal{V}} J_{ab} x_a x_b \right). \quad (3)$$

In what follows, we will focus on finding the Maximum-A-Posteriori (MAP) state of the IMP conditioned to a particular initialization – setting a subset of nodes, $\mathcal{I} \in \mathcal{V}$, to be infected. We coin the MAP problem **Inference Challenge**:

$$x^{(\text{MAP})}(\mathcal{I} | J, h) = \arg \min_x E(x | J, h) \Big|_{\forall a \in \mathcal{I}: x_a = +1}, \quad (4)$$

where we emphasize dependence of the MAP solution on the set of the initially infected nodes, \mathcal{I} .

Note that in general finding $x^{(\text{MAP})}$ is NP-hard (Barahona 1982). However if $J > 0$ element-wise, i.e. the Ising Model is attractive (also called ferromagnetic in statistical physics), Eq. (4) becomes equivalent to a tractable (polynomial in N) Linear Programming (see (Živný, Werner, and Průša 2014) and references therein). In fact, the IMP is attractive, reflecting the fact that the state of a node is likely to be aligned with the state of its neighbor.

Let us also emphasize some other features of the IMP:

1. \mathcal{G} should be thought of as an "interaction" graph of a city, reflecting transportation, commutes, and other forms of interactions between populations with the homes at the two nodes (census tracts) linked by an edge. The strength of a particular J_{ab} shows the level of interaction associated with the edge $\{a, b\}$.
2. A component, h_a , of the vector of local biases, h , is reflecting a -node specific factors such as immunization level, imposed quarantine, and degree of compliance with the public health measures (e.g., wearing masks and following other rules). Large negative/positive h_a shows that residents of the census tract associated with the node a are largely healthy/infected.

If solution of the Inference Challenge problem is such that the **R**-subset of the MAP solution, $x^{(\text{MAP})}(\mathcal{I} | J, h)$, i.e.

$$\mathcal{R}(\mathcal{I}, J, h) = \left\{ a \in \mathcal{V} | x_a^{(\text{MAP})}(\mathcal{I} | J, h) = +1 \right\}, \quad (5)$$

is sufficiently large, we would like to mitigate the infection, therefore setting the Prevention Challenge discussed in the next Section.

2 Prevention Challenge

Let us assume that modification of J and h are possible and consider the space of all feasible J and h . We will then identify *Safe Domain* as a sub-space of feasible J and h such that for all the initial sets of the initially infected nodes, \mathcal{I} , considered the resulting "infected" subset, $\mathcal{R}(\mathcal{I}, J, h)$, is sufficiently small. A more accurate definition of the Safe Domain follows. Then, we rely on the definition to formulate the control/mitigation problem coined Prevention Challenge. At this stage, we would also like to emphasize that studying the

geometry of the Safe Domain is one of the key contributions of this manuscript.

Definition. Consider IMP over $\mathcal{G} = (\mathcal{V}, \mathcal{E})$ and with the parameters (J, h) . Let us also assume that the set of initially infected nodes, \mathcal{I} , is drawn from the list, Υ . We say that (J, h) is in the k -Safe Domain if for every \mathcal{I} from Υ the number of \mathbf{R} -nodes in the MAP solution (4), is at most k , i.e.

$$\forall \mathcal{I} \in \Upsilon : |\mathcal{R}(\mathcal{I}, J, h)| \leq k, \quad (6)$$

where $\mathcal{R}(\mathcal{I}, J, h)$ is defined in Eq. (5).

Prevention Challenge: Given $(J^{(0)}, h^{(0)})$ describing the bare status of the system (city) which is not in the k -Safe Domain, and given the cost of the (J, h) change, $C((J, h); (J^{(0)}, h^{(0)}))$, what is least expensive change to $(J^{(0)}, h^{(0)})$ state of the system which is in the the k -Safe Domain? Formally, we are interested to solve the following optimization:

$$(J^{(\text{corr})}, h^{(\text{corr})}) = \arg \min_{(J, h)} C((J, h); (J^{(0)}, h^{(0)})) \quad \text{Eq. (6)} \quad (7)$$

Expressing it informally, the Prevention Challenge seeks to identify a minimal correction (thus "corr" as the upper index) $(J^{(\text{corr})}, h^{(\text{corr})})$, which will move the system to the safe regime from the unsafe bare one, $(J^{(0)}, h^{(0)})$. The measures may include limiting interaction along some edges of the graph, thus modifying some components of J , or enforcing local biases, e.g., increasing level of vaccination, at some component of h .

Given that condition in Eq. (6) also requires solving Eq. (4) for each candidate (J, h) , the **Prevention Challenge** formulation is a difficult two-level optimization. However, as we will see in the next Section, the condition in Eq. (6) (and thus the inner part of the aforementioned two-level optimization) can be re-stated as the requirement of being inside of a polytope in the (J, h) space. In other words, the (k) -Safe Domain is actually a polytope in the (J, h) space.

3 Geometry of the MAP States

Before solving the Prevention Challenge problem, we want to shed some light on the geometry of the MAP states. We work here in the space of all the Ising models over a graph $\mathcal{G} = (\mathcal{V}, \mathcal{E})$, where each of the models is specified by (J, h) .

Proposition. Safe Domain of a graph $\mathcal{G} = (\mathcal{V}, \mathcal{E})$ with $N = |\mathcal{V}|$ nodes is a polytope in the space of all feasible parameters, (J, h) , defined by an exponential in N number of linear constraints.

Remark. The Proposition allows us, from now on, to use *Safe Polytope* instead of the *Safe Domain*.

Proof of the Proposition. The space of all the Ising models is divided into 2^N regions by the corresponding MAP states. Moreover, the boundary between any pair of neighboring regions is linear: consider two states $x^{(i)}$ and $x^{(j)}$, and denote $(J, h)^{(i)}$ (resp. $(J, h)^{(j)}$) the set of all the Ising models with the MAP state $x^{(i)}$ (resp. $x^{(j)}$), then $(J, h)^{(i)}$ and $(J, h)^{(j)}$ are separated by the equation, $E(x^{(i)} | J, h) =$

$E(x^{(j)} | J, h)$, which is linear in (J, h) . For a subset, $R \subseteq \mathcal{V}$, of nodes, let $x^{(R)}$ be the state in which, $x_a = +1, \forall a \in R, x_a = -1, \forall a \notin R$. Let $X^{(R)}$ be the set of all the MAP states, x , such that $\forall a \in R, x_a = +1$ (while other nodes, i.e. $b \in \mathcal{V} \setminus R$, are not constrained, $x_b = \pm 1$). Then the k -Safe Polytope, which we denote, $\text{SP}(k)$, is defined by at most $\sum_{k'=1}^k \binom{N}{k'} \cdot (2^{N-k'} - 1)$ linear inequalities:

$$\text{SP}(k) = \bigcap \left\{ (J, h) \mid E(x^{(R)} | J, h) > E(x | J, h) \right\}, \quad (8)$$

$$\forall R, |R| \leq k; \quad \forall x \in X^{(R)} \setminus x^{(R)}$$

were some of these linear inequalities on the rand hand side may be redundant.

Remark. In the case of $k = 1$ (which, obviously, applies only if all the initial infections are at a single nodes, i.e. $\forall \mathcal{I} \in \Upsilon, |\mathcal{I}| = 1$), there are at most, $N \cdot (2^{N-1} - 1)$ linear inequalities.

We illustrate the geometry of the Ising model over the triangle graph (three nodes connected in a loop, K_3) in Fig. 2 and Fig. 3. For both illustrations, we fix the h value to -1 at all the nodes, and we are thus exploring the remaining three degrees of freedom, J_{12}, J_{13}, J_{23} (since J is symmetric), which corresponds to exploring interactions within the class of attractive Ising models, $\forall a, b = 1, 2, 3 : J_{ab} \in \mathbb{R}_+$.

First, we consider the case when the only node $a = 1$ is infected. In this simple setting there are four possible MAP states, $(x_1, x_2, x_3) \in \{(+1, -1, -1), (+1, -1, +1), (+1, +1, -1), (+1, +1, +1)\}$, shown in Fig. (2) as green, blue, yellow and red, respectively. Finally, in the figure Fig. (3) we plot the Safe Polytope $\text{SP}(1)$. We observe that the two "polarized" MAP states, $(+1, -1, -1)$ and $(+1, +1, +1)$, are seen most often among the samples, while domain occupied by the other two "mixed" MAP states, $(+1, -1, +1)$ and $(+1, +1, -1)$ is much smaller, with the two modes positioned on the interface between the two polarized states.

As will be shown below in the next Section, the polarization phenomena with only two "polarized" MAP states, which we coin in the following the two polarized modes, which we see on this simple triangle example, is generic for the attractive Ising model.

4 Two Polarized Modes

Definition. Consider a particular subset of the initially infected nodes, \mathcal{I} (where thus, $\forall a \in \mathcal{I} : x_a = +1$). We call the MAP state of the model *polarized* when one of the following is true: (i) only initially infected nodes show $+1$ within the MAP solution, $\forall a \in \mathcal{I} : x_a = +1, \forall b \in \mathcal{V} \setminus \mathcal{I} : x_b = -1$ or (ii) all nodes within the MAP state show $+1, \forall a \in \mathcal{V} : x_a = +1$. We call a MAP state *mixed* otherwise.

Experimenting with many dense graphs, which are typical in the pandemic modeling of modern cities with extended infrastructures and multiple destinations visited by many inhabitants, we observe that the two polarized MAP states dominate generically, while the mixed states are extremely rare.

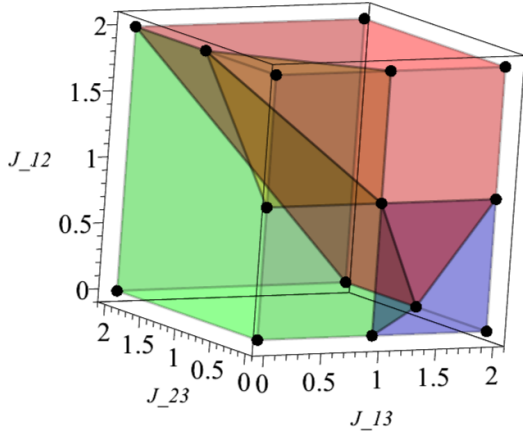


Figure 2: Geometry of the attractive Ising model illustrated on the example of a triangle graph (K_3) when a single node is infected. See explanations in the text.

Fig. 4 illustrates results of one our ensemble of random IMPs' experiments. We, first, fix N to 20, pick M such that $M \leq N(N-1)/2 = 190$ and then generate at random M edges connecting the 20 nodes. Then, for each of the random graphs (characterized by its own M) we generate 500 random samples of (J, h) , representing attractive Ising models. Finally, we find the MAP state for each IMP instance, count the number of mixed states and show the dependence of the fractions of the mixed states (in the sample set) in the Fig. (4). A fast decrease of the proportion of the mixed states is observed with an increase in M .

Extension of these experiments (see Fig. (5)) suggests that when we consider an ensemble of IMPs over graphs with N nodes and the average degree $\alpha = O(1)$ which is sufficiently large (so that the graph is sufficiently dense) and increase N , we observe that the Mixed State Probability (MSP), or equivalently proportion of the mixed-to-polarized states, decreases dramatically. Moreover, based on the experiments, we conjecture that the MSP decays to zero at $\alpha > \alpha_c$, but it saturates at $\alpha < \alpha_c$, where α_c is the threshold depending on the ensemble details. This threshold behavior is akin to the phase transition that occurred in many models of the spin glass theory (Mezard, Parisi, and Virasoro 1986) and many models of the Computer Science and Theoretical Engineering defined over random graphs and considered in the thermodynamic limit, i.e. at $N \rightarrow \infty$. See e.g. (Richardson and Urbanke 2008) (application in the Information Theory, and specifically in the theory of the Low Density Parity Check Codes) (Mezard and Montanari 2009) (applications in the Computer Science, and specifically for random SAT and related models) and references therein. We postpone further discussions of the conjecture for a future publication (see also brief discussion in Section 7).

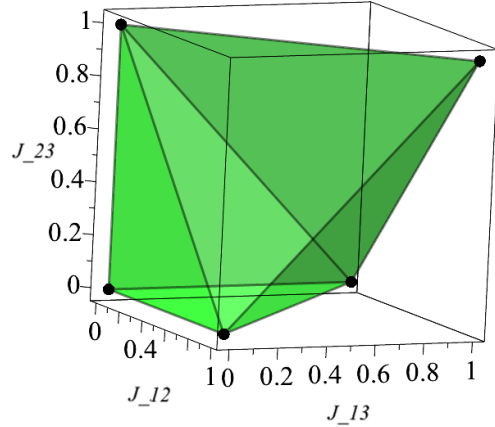


Figure 3: The Safe Polytope illustrated on the example of a triangle graph (K_3) with field vector $h = [-1, -1, -1]$. See explanations in the text.

We will continue discussion of the two-mode solution in the next Section.

5 Projecting to the Safe Polytope

In this Section we aim to summarize all the findings so far to resolve the Prevention Challenge formulated in Section 2, specifically in Eq. (7) stating the problem as finding a minimal projection to the Safety Domain/Polytope from its exterior. The task is well defined, but in general, and as shown in Section 3, it is too complex – as the description of the Safety Polytope (number of linear constraints, required to define it) is exponential in the system size (number of nodes in the graph). However, the two-mode approximation, introduced in Section 4, suggests a path forward: use the two-mode approximation and therefore remove all the linear constraints but one, separating the two polarized states.

Let us denote the two-mode approximation of the Safe Polytope by $\widehat{SP}(\Upsilon)$, where thus k in the original Safe Polytope, $SP(k)$, is replaced by the set Υ of all the initial infection patters. Then we write,

$$\widehat{SP}(\Upsilon) = \bigcap_{\mathcal{I} \in \Upsilon} \{(J, h) \mid E(+1^{2N} \mid J, h) \geq E(x^{\mathcal{I}} \mid J, h)\}, \quad (9)$$

where, $\forall a \in \mathcal{I} : x_a^{(\mathcal{I})} = +1$ and $\forall b \in \mathcal{V} \setminus \mathcal{I} : x_b^{(\mathcal{I})} = -1$. Eq. (9) represents a polytope stated in terms of the $|\Upsilon|$ constraints. In particular, if Υ accounts for all the initial infections, \mathcal{I} , of size not large than k , then $|\Upsilon| = \sum_{k'=1}^k \binom{N}{k'}$: the number of constraints grows exponentially in the maximal size of the initial infections, however the number of the constraints remains tractable for any $k = O(1)$. Replacing conditions in Eq. (7) by $\widehat{SP}(\Upsilon)$, defined in Eq. (9), one arrives at

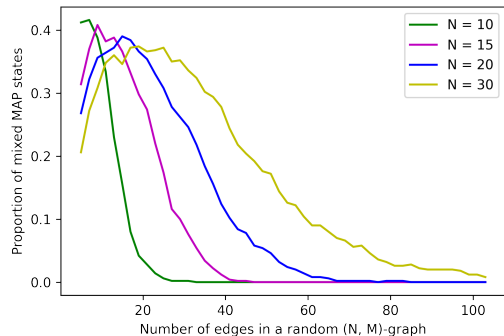


Figure 4: Proportion of the mixed states in all samples for an ensemble of the (attractive) Ising Model of Pandemic over graphs with N nodes, shown as a function of the varying number of edges, M . Each shown point is the result of the averaging over 500 random instances of the (J, h) over the same graph. (See text for additional details.)

the following tractable (in the case of $k = O(1)$) convex optimization expression answering the Prevention Challenge approximately (within the two-mode approximation):

$$(\hat{J}^{(\text{corr})}, \hat{h}^{(\text{corr})}) = \arg \min_{(J, h)} C\left((J, h); (J^{(0)}, h^{(0)})\right)_{\text{Eq. (9)}}. \quad (10)$$

This formula is the final result of this manuscript analytic evaluation. In the next Section we use Eq. (10), with $C(\cdot; \cdot)$ substituted by the l_1 -norm, to present the result of our experiments in a quasi-realistic setting describing a (hypothetical) pandemic attack and optimal defense, i.e., prevention scheme.

6 Experiments

Seattle data

We illustrate our methodology on a case study of the city of Seattle. Seattle has 131 Census Tracts. (Each Census Tract includes 1 to 10 Census Block Groups with 600 to 3000 residents.) Each Census Tract represents 1200 to 8000 population, and its boundaries are designed to represent natural or urban landmarks and also to be persistent over a long period (United States Census Bureau 2019). To reduce complexity, we merge census tracts into 20 regions. See Fig. 6. To prepare this splitting of Seattle into 20 regions/nodes, we utilize geo-spatial information from the TIGER/Line Shapefiles project provided by U.S. Census Bureau (United States Census Bureau 2021). The travel data of Seattle was extracted from the Safegraph dataset (Saf), which provides anonymized mobile tracking data. Each data point in the Safegraph database describes the number of visits from a Census Block to a specific point of interest represented by latitude and longitude. Mobility data associated with travelers crossing the boundaries of Seattle was ignored. We then follow the methodology developed in (Chertkov et al. 2021) to combine the aggregated travel data with the epidemiological data, representing current state of infection in the area.

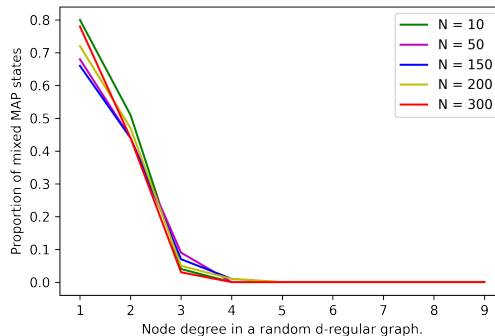


Figure 5: Proportion of the mixed-to-polarized states for an ensemble of the (attractive) Ising Model of Pandemic over d -regular graphs with N nodes, shown as a function of d . Each point is the result of averaging over 100 random instances of the (J, h) over different random graphs with the same node degree. (See text for additional details.)

This results in the estimation of the pair-wise interactions, J , parameterizing the Ising Model of Pandemic. We also come up with an exemplary (uniform over the system) local biases, h , completing the definition of the model. (We remind that the prime focus of the manuscript is on developing methodology which is AI sound and sufficiently general. Therefore, the data used in the manuscript are roughly representative of the situation of interest, however not fully practical.) We consider a situation with different levels of infection and chose $(J^{(0)}, h^{(0)})$ stressed enough, that is resulting in the prediction (answer to our Prediction Challenge), which lands the system in the dangerous domain – outside of the Safety Polytope.

Convex projection

In all of our experiments, we have used the general-purpose Gurobi optimization solver (Gurobi Optimization, LLC 2021) to compute the MAP states and thus to validate the two-mode assumption. (We have also experimented with CVXPY (CVXPY 2021), but found it performing slower than Gurobi, at least over the relatively small samples considered in this proof of principles study. In the future, we plan to use existing, or developing new, LP solvers designed specifically for finding the MAP state of the attractive Ising model.) To illustrate our Prevention strategy, we took the Seattle data described above, and fed it as an input into the optimization (10), describing projection to the Safety Polytope, where $C(\cdot; \cdot)$ is substituted by the l_1 norm. CVXPY solver was used for this convex optimization task. Our code (python within jupyter notebook) is available at <https://github.com/mkrechetov/IsingMitigation>.

Table 1 shows results of our Prevention experiments on the Seattle data. We analyze l_1 projection to $\overline{SP}(\Upsilon)$ where Υ consists of all the initial infection patterns consisting of up to k nodes. In all of our experiments, the values of the field vector h (uniform across the system) was fixed to -1 . We observe that the number of constraints grows exponentially

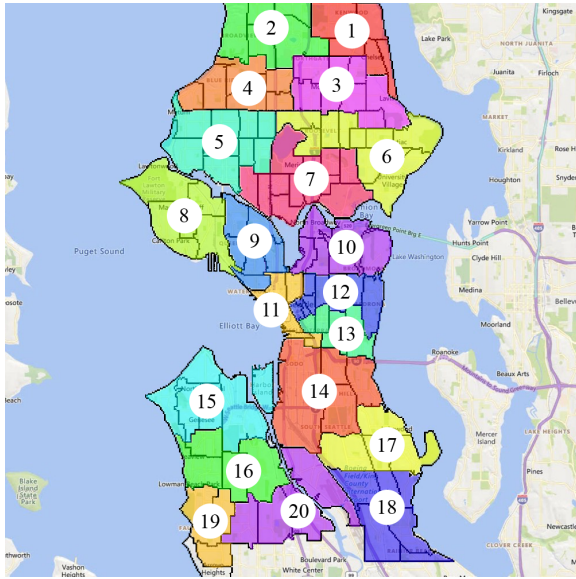


Figure 6: Seattle case study areas and census tracts (Office of Planning & Community Development, Seattle 2010).

k	LP Constraints	Runtime	Cost
1	801	1.65s	41.69
2	991	3.04s	43.62
3	2131	10.90s	44.30
4	6976	100.08s	44.56

Table 1: Summary of our prevention experiments on the Seattle data. k , in the first column, is the maximal number of nodes in the initially infected patterns (all accounted for to construct the k -Safe Polytope). The second column shows number of linear constraints characterizing the k -Safe Polytope. Respective Run Time and Cost are shown in the 3rd and 4th column, where Cost shows the difference in l_1 norm between the $(J^{(0)}, h^{(0)})$, characterizing stressed but unmitigated regime, and the optimal prevention regime, resulting in $(\hat{J}^{(\text{corr})}, \hat{h}^{(\text{corr})})$ computed according to Eq. (10).

with k ; however, the cost of intervention remains roughly the same. We intend to analyze the results of this and other (more realistic) experiments in future publications aimed at epidemiology experts and public health officials.

7 Conclusions and Path Forward

In this manuscript, written specifically for the AI community, we follow our prior work (Chertkov et al. 2021), aimed at a broader interdisciplinary community, and explain respective inference (prediction) and control (prevention) questions/challenges. We use the language of GMs, which is one powerful tool in the modern arsenal of AI, and state the Prediction Challenge as a MAP optimization over an attractive Ising model, which can be expressed generically as a solution of a tractable Linear Programming (LP). We then turn to the analysis of the prevention problem, which is set if the aforementioned prediction solution suggests that the

probability of significant infection is above a pre-defined (by the public health experts) tolerance threshold. We show that in its simplest formulation, the prevention problem is equivalent to finding minimal l_1 projection to the safety polytope, where the latter is defined by solving the aforementioned prediction problem. In general, the polytope does not allow a description non-exponential in the size of the system. However, we suggested an approximation that allows to approximate the safety polytope efficiently - that is, linearly in the number of the initial infection patterns. The approximation is justified (empirically, with supporting theoretical arguments, however not yet backed by a mathematically rigorous theory) in the case when the interaction graph of the system (e.g., related to the system/city transportation and human-to-human interaction network) is sufficiently dense. We conclude by providing a quasi-realistic experimental demonstration on the GM of Seattle.

We conclude the manuscript with an incomplete list of AI challenges, presented in the order of importance (subjective), which need to be resolved to make the powerful GM approach to pandemic prediction and prevention practical:

- Build a hierarchy of Probabilistic Graphical Models which allow more accurate (than Ising model) representation of the infection patterns over geographical and community graphs. The models may be both of the static (like Ising) or dynamic (like Independent Cascade Model) types. Extend the notion of the Safety Region (polytope) to the new GM of pandemics.
- Consider the case when the resolution of the Prediction Challenge problem returns a positive answer - most likely future state of the system is safe, and then develop the methodology which allows estimating the probability of crossing the safety boundary. In other words, we envision formulating and solving in the context of the GM a problem which is akin to the one addressed in (Owen, Maximov, and Chertkov 2019): estimate the probability of finding the system outside of the Safety Polytope.
- Construct other (than two-mode) approximations to the Safety Polytope. Approximations built on sampling of the boundaries of the safety polytope and learning (possibly reinforcement learning) are needed.
- Develop the asymptotic (thermodynamic limit) theory which allows validating (and/or correcting systematically) the efficient (two-mode and other) approximations of the Safety Polytope.

Acknowledgments

This work was supported in part by NSF via #2027072 "RAPID:Infer and Control Global Spread of Corona-Virus with Graphical Models" project.

References

- ???? SafeGraph COVID-19 Data Consortium. San Francisco, CA: SafeGraph Inc.
- Anderson, R.; and May, R. 1991. *Infectious Disease of Humans: Dynamics and Control*. Oxford University Press, Oxford.
- Barahona, F. 1982. On the computational complexity of Ising spin glass models. *Journal of Physics A: Mathematical and General*, 15(10): 3241–3253.
- Chang, S.; Pierson, E.; Koh, P. W.; Gerardin, J.; Redbird, B.; Grusky, D.; and Leskovec, J. 2020. Mobility network models of COVID-19 explain inequities and inform reopening. *Nature*.
- Chao, D. L.; Halloran, M. E.; Obenchain, V. J.; and Longini Jr, I. M. 2010. FluTE, a publicly available stochastic influenza epidemic simulation model. *PLoS Comput Biol*, 6(1): e1000656.
- Chen, Y.-C.; Lu, P.-E.; Chang, C.-S.; and Liu, T.-H. 2020. A Time-Dependent SIR Model for COVID-19 With Undetectable Infected Persons. *IEEE Transactions on Network Science and Engineering*, 7(4): 3279–3294.
- Chertkov, M.; Abrams, R.; Esmiaeeli Sikaroudi, A. M.; Krechetov, M.; Slagle, C.; Efrat, A.; Fulek, R.; and Oren, Y. 2021. Graphical Models of Pandemic. <https://www.medrxiv.org/content/10.1101/2021.02.24.21252390v1.full>.
- CVXPY. 2021. Convex Optimization for Everyone. <https://www.cvxpy.org/>.
- Downey, A. 2018. *Think Complexity: Complexity Science and Computational Modeling*. O’Reilly Media, Inc., 2nd edition. ISBN 1549761749.
- Eubank, S.; Eckstrand, I.; Lewis, B.; Venkatramanan, S.; Marathe, M.; and Barrett, C. L. 2020. Commentary on Ferguson, et al., “Impact of Non-pharmaceutical Interventions (NPIs) to Reduce COVID-19 Mortality and Healthcare Demand”. *Bulletin of Mathematical Biology*, 82(4): 52.
- Eubank, S.; Guclu, H.; Anil Kumar, V. S.; Marathe, M. V.; Srinivasan, A.; Toroczkai, Z.; and Wang, N. 2004. Modelling disease outbreaks in realistic urban social networks. *Nature*, 429(6988): 180–184.
- Ferguson, N.; Laydon, D.; Nedjati-Gilani, G.; Imai, N.; Ainslie, K.; Baguelin, M.; Bhatia, S.; Boonyasiri, A.; Cucunubá, Z. M.; Cuomo-Dannenburg, G.; Dighe, A.; Dorigatti, I.; Fu, H.; Gaythorpe, K.; Green, W.; Hamlet, A.; Hinsley, W.; Okell, L.; van Elsland, S.; and Ghani, A. 2020. Report 9: Impact of non-pharmaceutical interventions (NPIs) to reduce COVID-19 mortality and healthcare demand. <https://www.imperial.ac.uk/media/imperial-college/medicine/sph/ide/gida-fellowships/Imperial-College-COVID19-NPI-modelling-16-03-2020.pdf>.
- Ferguson, N. M.; Cummings, D. A.; Cauchemez, S.; Fraser, C.; Riley, S.; Meeyai, A.; Iamsirithaworn, S.; and Burke, D. S. 2005. Strategies for containing an emerging influenza pandemic in Southeast Asia. *Nature*, 437(7056): 209–214.
- Ferguson, N. M.; Cummings, D. A. T.; Fraser, C.; Cajka, J. C.; Cooley, P. C.; and Burke, D. S. 2006. Strategies for mitigating an influenza pandemic. *Nature*, 442(7101): 448–452.
- Germann, T. C.; Kadau, K.; Longini, I. M.; and Macken, C. A. 2006. Mitigation strategies for pandemic influenza in the United States. *Proceedings of the National Academy of Sciences*, 103(15): 5935–5940.
- Gomez-Rodriguez, M.; Leskovec, J.; and Krause, A. 2012. Inferring Networks of Diffusion and Influence. *ACM Trans. Knowl. Discov. Data*, 5(4).
- Gurobi Optimization, LLC. 2021. Gurobi Optimizer Reference Manual. <https://www.gurobi.com>.
- Halloran, M. E.; Ferguson, N. M.; Eubank, S.; Longini, I. M.; Cummings, D. A. T.; Lewis, B.; Xu, S.; Fraser, C.; Vullikanti, A.; Germann, T. C.; Wagener, D.; Beckman, R.; Kadau, K.; Barrett, C.; Macken, C. A.; Burke, D. S.; and Cooley, P. 2008. Modeling targeted layered containment of an influenza pandemic in the United States. *Proceedings of the National Academy of Sciences*, 105(12): 4639–4644.
- Hethcote, H. W. 2000. The Mathematics of Infectious Diseases. *SIAM Rev.*, 42(4): 599–653.
- Kaxiras, E.; and Neofotistos, G. 2020. Multiple Epidemic Wave Model of the COVID-19 Pandemic: Modeling Study. *Journal of Medical Internet Research*, 22(7): e20912.
- Kempe, D.; Kleinberg, J.; and Tardos, E. 2003. Maximizing the Spread of Influence through a Social Network. In *Proceedings of the Ninth ACM SIGKDD International Conference on Knowledge Discovery and Data Mining, KDD ’03*, 137–146. New York, NY, USA: Association for Computing Machinery. ISBN 1581137370.
- Kermack, W. O.; McKendrick, A. G.; and Walker, G. T. 1927. A contribution to the mathematical theory of epidemics. *Proceedings of the Royal Society of London. Series A, Containing Papers of a Mathematical and Physical Character*, 115(772): 700–721.
- Kerr, C. C.; Stuart, R. M.; Mistry, D.; Abeyesuriya, R. G.; Rosenfeld, K.; Hart, G. R.; Nunez, R. C.; Cohen, J. A.; Selvaraj, P.; Hagedorn, B.; George, L.; Jastrzebski, M.; Izzo, A. S.; Fowler, G.; Palmer, A.; Delport, D.; Scott, N.; Kelly, S. L.; Bennette, C. S.; Wagner, B. G.; Chang, S. T.; Oron, A. P.; Wenger, E. A.; Panovska-Griffiths, J.; Famulare, M.; and Klein, D. J. 2021. Covasim: An agent-based model of COVID-19 dynamics and interventions. *PLOS Computational Biology*, 17(7): 1–32.
- Khalil, E. B.; Dilkina, B.; and Song, L. 2013. CuttingEdge: Influence minimization in networks. In *Workshop on Frontiers of Network Analysis: Methods, Models, and Applications at NIPS*.
- LANL. 2020. COVID-19 Confirmed and Forecasted Case Data. <https://covid-19.bsvgateway.org/>.
- Longini, I.; Nizam, A.; Xu, S.; Ungchusak, K.; Hanshaworakul, W.; Cummings, D.; and Halloran, M. 2005. Containing pandemic influenza at the source. *Science*, 309(5737): 1083–1087.
- Lovasi, G.; and et.al. 2020. Population Health Methods: Agent Based Modeling.
- Maziarz, M.; and Zach, M. 2020. Agent-based modelling for SARS-CoV-2 epidemic prediction and intervention assessment: A methodological appraisal. *Journal of Evaluation in Clinical Practice*, 26(5): 1352–1360.

Mezard, M.; and Montanari, A. 2009. *Information, Physics, and Computation*. USA: Oxford University Press, Inc. ISBN 019857083X.

Mezard, M.; Parisi, G.; and Virasoro, M. 1986. *Spin Glass Theory and Beyond*. WORLD SCIENTIFIC.

Netrapalli, P.; and Sanghavi, S. 2012. Learning the Graph of Epidemic Cascades. In *Proceedings of the 12th ACM SIGMETRICS/PERFORMANCE Joint International Conference on Measurement and Modeling of Computer Systems*, SIGMETRICS '12, 211–222. New York, NY, USA: Association for Computing Machinery. ISBN 9781450310970.

Office of Planning & Community Development, Seattle. 2010. Census tract map of Seattle, <https://www.seattle.gov/Documents/Departments/OPCD/Demographics/GeographicFilesandMaps/2010CensusTractMap.pdf>.

Owen, A. B.; Maximov, Y.; and Chertkov, M. 2019. Importance sampling the union of rare events with an application to power systems analysis. *Electronic Journal of Statistics*, 13(1): 231 – 254.

Richardson, T.; and Urbanke, R. 2008. *Modern Coding Theory*. USA: Cambridge University Press. ISBN 0521852293.

Rosenfeld, N.; Nitzan, M.; and Globerson, A. 2016. Discriminative Learning of Infection Models. In *Proceedings of the Ninth ACM International Conference on Web Search and Data Mining*, WSDM '16, 563–572. New York, NY, USA: Association for Computing Machinery. ISBN 9781450337168.

Ross, R. 1910. *The Prevention of Malaria*. John Murray, London.

SafeGraph. 2021. SafeGraph Social Distancing Metrics. San Francisco, CA: SafeGraph Inc., <https://docs.safegraph.com/docs/social-distancing-metrics>.

United States Census Bureau. 2019. United States Census Bureau glossary, <https://www.census.gov/programs-surveys/geography/about/glossary.html>.

United States Census Bureau. 2021. United States Census Bureau. TIGER Line shapefiles Technical documentation.

Wikipedia. 2020. Agent Based Models, https://en.wikipedia.org/wiki/Agent-based_model.

Živný, S.; Werner, T.; and Průša, D. a. 2014. The Power of LP Relaxation for MAP Inference. *Advanced Structured Prediction, The MIT Press*, 19–42.